Determination of food additive zinc-cobalt(II) phosphate form resistant to high temperatures

Nadiia Antraptseva[1], Olena Podobii[2], Galyna Bila[2]

1 – National University of Life and Environmental Sciences of Ukraine, Ukraine
2 – National University of Food Technologies, Kyiv, Ukraine

Keywords:

Phosphates
Zinc
Cobalt
Heat treatment
Dehydration

Article history:

Received 16.11.2022
Received in revised form 04.03.2023
Accepted 30.06.2023

Corresponding author:

Olena Podobii
E-mail: o.podobiy@gmail.com

DOI:
10.24263/2304-974X-2023-12-2-10

Abstract

Introduction. The aim of the research was to study the process of dehydration of zinc-cobalt(II) phosphates during heat treatment.

Materials and methods. Zinc-cobalt(II) phosphate tetrahydrates were used as the main research objects. The content of ingredients in the composition of phosphates was as follows, % mass.: Zn, 41.8–23.5; Co, 2.3–12.8; P, 13.6–13.8; H_2O, 16.1–16.3. Spectral methods were used to study the process and products of dehydration. Infrared absorption spectra were recorded at 20 °C and –190 °C, as well as in the process of heating phosphates. X-ray phase analysis was performed.

Results and discussion. In the structure of zinc-cobalt(II) phosphates there are two types of crystallographically non-identical water molecules, the OH groups of which form a rigid system of hydrogen bonds of different strength and directionality (from 29.35-30.48 kJ·mol^{-1} in the OH···OPO_3 group to 12.48–13.31 kJ·mol^{-1} in the OH···H_2O group). The energy of H-bonds, cation-water bonds and the asymmetry of water molecules increase with an increase in the cobalt content from 2.3 to 12.8 % mass., which is associated with a stronger polarizing effect of cobalt on water molecules that make up the nearest coordination environment of the cation. Zinc-cobalt(II) phosphates are thermally stable up to 85–90 °C. Upon further increase of temperature, their dehydration occurs with the pairwise removal of four water molecules and the formation of one hydrated form as an intermediate product – zinc-cobalt phosphate dihydrate. The temperature regimes of the process of dehydration of phosphates of different cationic composition correlate with the energy state of water molecules and are maximal in phosphate containing 12.8 % mass. cobalt. It is stable during heat treatment up to 90 °C. In the interval from 90 to125°C two water molecules are removed with the formation of zinc-cobalt (II) phosphate dihydrate. This compound is stable in the temperature interval from 125 to 250 °C. A further increase in temperature is accompanied by the release of the last two moles of water and the formation of completely dihydrated zinc-cobalt(II) phosphate. Temperature intervals of thermal stability of zinc-cobalt(II) phosphates and products of their dehydration are by 15–20 °C higher than phosphates with a higher cobalt content.

Conclusions. Zinc-cobalt(II) phosphate, containing the maximum amount of cobalt, is the most termostable form. Zinc-cobalt(II) phosphate dihydrate formed as a result of the release of two water molecules at 90–125 °C is the only stable product.

Introduction

Production of food with an increased content of microelements is an effective way to compensate their deficiency in the human diet (Damodaran et al., 2012; Stabnikova et al., 2021). The one of the most common methods to obtain food products enriched with microelements is their supplementing with individual salts or their mixtures (Damodaran et al., 2012). The use of phosphates of zinc, cobalt, manganese, magnesium, iron, calcium, and potassium to enhance food nutritional quality is known (Miller, 2010, 2017; Zimmermann et al., 2011). Phosphates are more often used to improve the quality meat and chicken products, as well as seafood (Bach, et al., 2011).

It was shown that the presence of phosphates in the meat products stabilized the pH value (Xu et al., 2021), increased the moisture-holding capacity, reduced the loss of moisture during the preparation, and improved the taste of the finished product (Wang, 2009). An improvement of the sensory properties of the finished product was also found in the case of adding 0.2% phosphate to chicken sausage (Stabnikova et al., 2022). A reduction of phosphate content leads to increasing cooking loss, and a deterioration of sensory properties of the finished meat products (Pinton et al., 2019).

Most technological processes of food preparation include heat treatment. Under heating the properties of treated material change, namely the moisture content and composition, not only of the raw materials, but also of additives that were incorporated in food product to enhance its nutrition value (Shao et al., 2016). To preserve the useful properties of biologically active additives, knowledge of the temperature ranges of their stability, the composition and properties of the products formed during their heat treatment is necessary.

Thermal properties of hydrated phosphates are determined by the energy state of water molecules included in their crystal lattice (Antraptseva et al., 2020). Therefore, the correct choice of the heat treatment mode of raw materials with the addition of phosphates of trace elements is possible only taking into account the process of their dehydration (Tiwari et al., 2015).

Knowledge about the processes occurring with phosphates of microelements used as additives during thermal processing of food, as well as information about the products formed from them under heating is extremely limited (Bila et al., 2016). As for zinc-cobalt phosphates, it is known that during heating they gradually lose water of crystallization with the formation of partially dihydrated phosphates (Bach et al., 2015). The formation of other hydrate forms and rehydration processes, which change the entire dehydration process, have not yet been studied.

The purpose of this work is to investigate the process and products of dehydration of food additive zinc-cobalt(II) phosphates during heat treatment.

Materials and methods

Zinc-cobalt(II) phosphates of the general formula $Zn_{3-x}Co_x(PO_4)_2 \cdot 4H_2O$ ($0<x\leq1.00$), in particular, $Zn_2Co(PO_4)_2 \cdot 4H_2O$, phosphate of the composition $Zn_{2.5}Co_{0.5}(PO_4)_2 \cdot 4H_2O$ and $Zn_3(PO_4)_2 \cdot 4H_2O$ was used as research objects. The content of ingredients in their composition varies within the range, % mass.: Zn, 41.8–23.5; Co, 2.3–12.8; P, 13.6–13.8; H_2O, 16.1–16.3.

Zinc hydroxocarbonate, ACS reagent; cobalt hydroxocarbonate, ACS reagent; phosphoric acid, ACS reagent; magnesium sulfate $MgSO_4 \cdot 7H_2O$, purified grade; manganese(II) sulfate $MnSO_4 \cdot 5H_2O$, purified grade; cobalt(II) sulfate $CoSO_4 \cdot 7H_2O$, purified

grade; zinc sulfate $ZnSO_4 \cdot 7H_2O$, purified grade, were used as initial substances for synthesis zinc-cobalt(II) phosphates.

Synthesis Zinc-cobalt(II) phosphates

The synthesis of zinc phosphate tetrahydrate and zinc-cobalt(II) phosphates was carried out by the interaction of a mechanical mixture of hydroxocarbonates of zinc and cobalt(II) with a solution of phosphoric acid, using recommendations of (Antraptseva et al., 2022). For this, a 45–87% H_3PO_4 solution was added to a reaction vessel thermostated at 40–70 °C containing distilled water until the pH was within 2.9–3.1. A homogenized mixture of zinc hydroxocarbonates with a zinc oxide ZnO content of 77.25 % mass. and cobalt with a CoO content of 68.32 % mass. was added to the resulting solution in parallel with constant stirring (ratio K = Zn/Co = 50.0–2.0, atomic) and a 45–87% H_3PO_4 solution maintaining pH 2.9–3.1. The precipitate was filtered, washed with water, dried at 40 °C and analysed. The characteristics of the received phosphates are given in the Table 1.

Table 1

Characteristics of the obtained zinc-cobalt(II) phosphates (55% H_3PO_4, 70 °C)

K = Zn/Co, atomic	Composition of phosphates, % mass.				Chemical composition	Phase composition (according to the results of X-ray and IR spectroscopy)
	Zn	Co	P	H_2O		
10.00	42.61	-	13.52	15.70	$Zn_3(PO_4)_2 \cdot 4H_2O$*	$Zn_3(PO_4)_2 \cdot 4H_2O$
9.00	30.73	4.62	13.72	16.19	$Zn_{2.63}Co_{0.37}(PO_4)_2 \cdot 4H_2O$	Phase composition $Zn_{3-x}Co_x(PO_4)_2 \cdot 4H_2O$ ($0<x\leq1.00$) structures $Zn_3(PO_4)_2 \cdot 4H_2O$
4.00	28.29	7.54	13.76	16.20	$Zn_{2.41}Co_{0.59}(PO_4)_2 \cdot 4H_2O$	
2.33	24.49	11.65	13.75	16.32	$Zn_{2.10}Co_{0.90}(PO_4)_2 \cdot 4H_2O$	
2.00	23.46	12.84	13.78	16.30	$Zn_{2.00}Co_{1.00}(PO_4)_2 \cdot 4H_2O$	

Note: * zinc phosphate obtained under these conditions contains Zn, P, H_2O, the content of which corresponds to the known calculated values for $Zn_3(PO_4)_2 \cdot 4H_2O$ (Antraptseva et al., 2022).

Chemical analysis

Phosphorus content was determined similarly (Antraptseva et al., 2022) by the weight quinolinemolybdate method (error 0.2 % relative). The total content of Zn^{2+} and Co^{2+}–cations by complexonometric titration (back titration, trilon B, standard zinc sulfate solution, eriochrome black T indicator, ammonia buffer solution with pH 10.0) analysis error 3 % relative (Scoog et al., 1992). The content of Co^{2+} was by the spectrophotometric method (Spectrophotometer SF–46, light absorption wavelength λ = 510 nm) in the form of a complex with surfactant (1-(2-pyridylazo)-resorcinol). The pH of the solution is 6.5–9.0 (citrate-ammonia buffer solution), the optimal concentration of cobalt ions – 0.1–4.0μg·ml^{-1}, the optimal concentration of surfactant is 60 μg·ml^{-1}, the error is 0.5% relative (Antraptseva et al., 2022). The zinc content was calculated as the difference between the sum of cations and the content of Co^{2+}. Water content was according to the loss of mass of samples when heated to 800 °C, determination error 1% relative (Derivatograph Q-1500 D).

Physico-chemical analysis

Spectral methods. IR absorption spectra were recorded at 20 °C and –190 °C in the frequency range 400-4000 cm^{-1}, as well as in the process of heating phosphates (Spectrometers Nexus – Nicolet 470 with Fourier transform and software Omnic and Specord 75 JR).

X-ray phase analysis. X-ray diffraction patterns were recorded using a DRON-4-M X-ray diffractometer in continuous shooting mode using Cu K_α, Fe K_α radiation. The speed of movement of the counter was 1 degree·min^{-1}. In order to reduce the systematic error, an internal standard was introduced – NaCl.

X-ray structural analysis was performed by full-profile analysis according to the Rietveld method using the FullProf Suite software package. For this, we used an array of diffraction data obtained from radiographs taken in the range of angles from 15 to 140° (2θ). The scanning step was 0.05°.

The thermal properties were studied in the temperature range of 25–900 °C under the conditions of dynamic and quasi-isothermal (labyrinth crucible, heating rate 3.0 degree·min^{-1}.) heating regimes (Derivatograph Q-1500 D).

Study of the process and products of dehydration of zinc-cobalt(II) phosphates

Spectral methods as are IR and CR spectroscopy, which are recognized as the most widespread and informative for assessing the state of OH groups and their functional connection in the crystal lattice of crystal hydrates, were chosen as the main research methods (Nakamoto, 2009).

Spectral studies were performed using two different IR spectroscopic techniques. According to the first of them, IR spectra of tetrahydrates and products of their partial and complete dehydration were recorded at 20 °C and –190 °C in the range of 400–4000 cm^{-1} on Specord-75 IR and Nexus-470 spectrometers with Fourier transform and software Omnic. The samples were prepared by pressing a fixed amount (0.05 % mass.) into a KBr matrix as in article (Koleva et al., 2019). The absorption spectra in the region corresponding to the oscillations of the water of crystallization (1400–4000 cm^{-1}) were obtained using a suspension of phosphates in butyl alcohol applied to a neutral fluorite substrate. Vaseline oil was added to the suspension to improve band resolution and reduce the overall absorption background.

The according to the second method, recording of IR spectra was used during the heating of the samples. Measurements of zinc-cobalt(II) tetrahydrate phosphates were ground with butyl alcohol, the suspension was applied to a neutral fluorite substrate. After drying the sample, the substrate was placed in the oven, which was in the cuvette compartment of the spectrophotometer, and heated. Dehydration of hydrated phosphate was assessed by changes in the intensity of absorption bands of valence vibrations of water molecules during heating.

Changes in the intensity of the ν(OH) absorption bands during heating were recorded in two ways. First, the spectrum was recorded at a constant frequency corresponding to the maximum of the absorption band being studied, while fixing the heating temperature. After each sharp drop in intensity, which was registered by the deviation of the curve from horizontality and the appearance of steps of different heights, the spectrum was recorded in the entire absorption range of ν(OH) – 3700-3000 cm^{-1} at a temperature corresponding to the step under consideration. If in the spectrum of the original tetrahydrate, the valence vibrations of the OH-groups of water molecules were characterized by several maxima, then the changes in the intensity of each of them were studied separately.

The use of this technique of spectroscopic study of the dehydration of crystal hydrates made it possible to trace the sequence of water removal and the formation of all intermediate hydrate forms, including those unstable at room temperature.

Results and discussion

State of water molecules and phosphate anion in the structure of zinc-cobalt(II) phosphates

The state of water molecules in the structure of zinc-cobalt(II) phosphates

Analysis of the IR spectra of zinc-cobalt(II) phosphates of composition $Zn_2Co(PO_4)_2 \cdot 4H_2O$, $Zn_{2.5}Co_{0.5}(PO_4)_2 \cdot 4H_2O$, the phosphate-matrix, $Zn_3(PO_4)_2 \cdot 4H_2O$, and their deuteroanalogues was writing at 20 °C and –190 °C (Figure 1) shows that at room temperature in the region of valence vibrations of OH groups of water molecules (3000–3600 cm^{-1}) (Nakamoto, 2009), two absorption bands are observed (the values of their maxima are given in Table 2) and one – in the region of deformation vibrations (1550–1750 cm^{-1}).

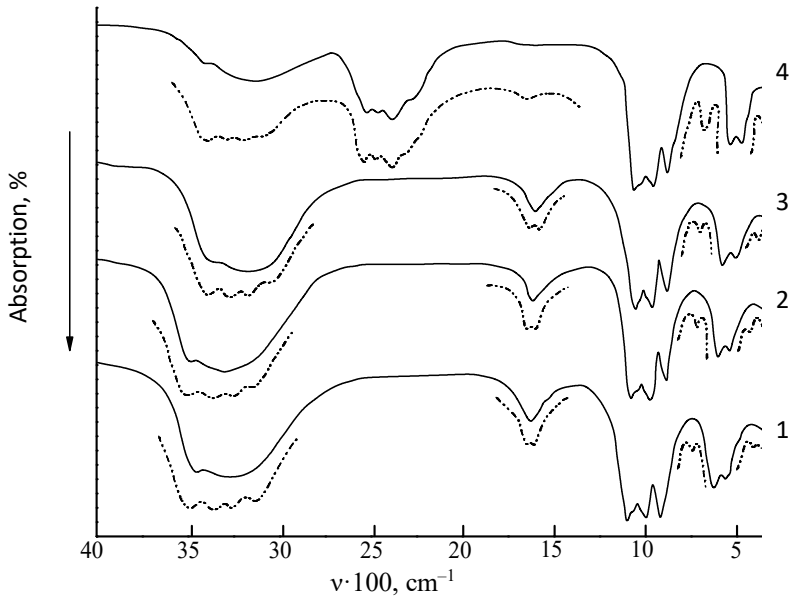

Figure 1. IR absorption spectra of $Zn_3(PO_4)_2 \cdot 4H_2O$ (1), $Zn_{2.5}Co_{0.5}(PO_4)_2 \cdot 4H_2O$ (2), $Zn_2Co(PO_4)_2 \cdot 4H_2O$ (3), $Zn_2Co(PO_4)_2 \cdot 4D_2O$ (4), recorded at 25 °C and –190 °C (marked with a dotted line)

At the temperature of liquid nitrogen, four maxima are clearly registered in the range of valence oscillations, and two in the area of strain oscillations, which indicate the presence of non-equivalent types of water molecules in their structure (Antraptseva et al., 2020).

The study of the IR spectrum of the deuteroanalogue of the composition $Zn_2Co(PO_4)_2 \cdot 4D_2O$ made it possible to reliably identify the absorption bands due to the

presence of librational vibrations of water molecules, which indicate their rigid attachment to both Oxygen and Hydrogen (Bernardino et al., 2022). The nature of the configurations of the ν(OH) absorption bands also indicates the presence of hydrogen bonds in the structure of zinc-cobalt phosphates (Figure 1, Table 2).

Table 2

Characteristics of H-bonds in the structure of zinc-cobalt(II) phosphates

Composition of phosphates	Wave numbers of absorption band maxima ν(OH), cm^{-1}		Characteristics of H-bonds		
			E, $kJ \cdot mol^{-1}$		
			$OH \cdots OPO_3$	$OH \cdots H_2O$	R $O \cdots O$, nm $(PO_4)O \cdots O(H_2O)$
$Zn_{2.80}Co_{0.20}(PO_4)_2 \cdot 4H_2O$	3264	3518	29.35	12.48	0.274
$Zn_{2.60}Co_{0.40}(PO_4)_2\ 4H_2O$	3260	3515	29.41	12.51	0.274
$Zn_{2.50}Co_{0.50}(PO_4)_2 \cdot 4H_2O$	3254	3510	29.50	12.60	0.274
$Zn_{2.30}Co_{0.70}(PO_4)_2 \cdot 4H_2O$	3247	3504	30.34	12.94	0.274
$Zn_{2.20}Co_{0.80}(PO_4)_2 \cdot 4H_2O$	3244	3503	30.36	12.96	0.274
$Zn_{2.00}Co_{1.00}(PO_4)_2 \cdot 4H_2O$	3240	3500	30.48	13.31	0.274

The simultaneous presence of narrow high-frequency and wide low-frequency absorption bands in the spectra of zinc-cobalt phosphates indicates the different loading of each OH-group of water molecules and their participation in the formation of H-bonds of different strength and direction. This is consistent with the results of a study of IR spectra of cobalt phosphates (Koleva et al., 2019).

A comparative analysis of the IR spectra of phosphates with different contents of zinc and cobalt(II) shows that the frequencies of valence vibrations of OH-groups of water molecules depend on the ratio of zinc and cobalt in the octahedral of the phosphate crystal structure. With an increase in the content of cobalt(II) in the coordination polyhedron, there is a natural shift of the maxima of the ν(OH) absorption bands to the low-frequency region, both in the $M^{2+} - OH_2 \cdots OPO_3$ group and in the $M^{2+} - OH_2 \cdots OH_2$ group. It is especially clearly registered in the IR spectra of samples deposited on CaF_2 (Figure 2 a).

For $Zn_3(PO_4)_2 \cdot 4H_2O$, the maximum of the long-wave band corresponds to the frequency of 3280 cm^{-1}; for phosphates, in which half of the octahedral are filled with cobalt ($Zn_{2.5}Co_{0.5}(PO_4)_2 \cdot 4H_2O$), a broad maximum of 3180–3300 cm^{-1} is noted; replacing zinc with cobalt in all octahedral positions ($Zn_2Co(PO_4)_2 \cdot 4H_2O$) leads to a shift of ν(OH) to a frequency of 3150 cm^{-1}. A similar effect is also mentioned in the study (Petersen et al., 2022; Wu et al., 2015).

The energy of hydrogen bonds, estimated according to (Bartl, 2009) according to this shift, increases when going from $Zn_3(PO_4)_2 \cdot 4H_2O$ to $Zn_2Co(PO_4)_2 \cdot 4H_2O$. At the same time, the difference in the charge of OH-groups in the same water molecule also increases (Table 2). This is consistent with work (Grabowski, 2016) and is explained by the stronger polarizing effect of cobalt on water molecules that make up the nearest coordination environment of the cation (Petersen et al., 2022).

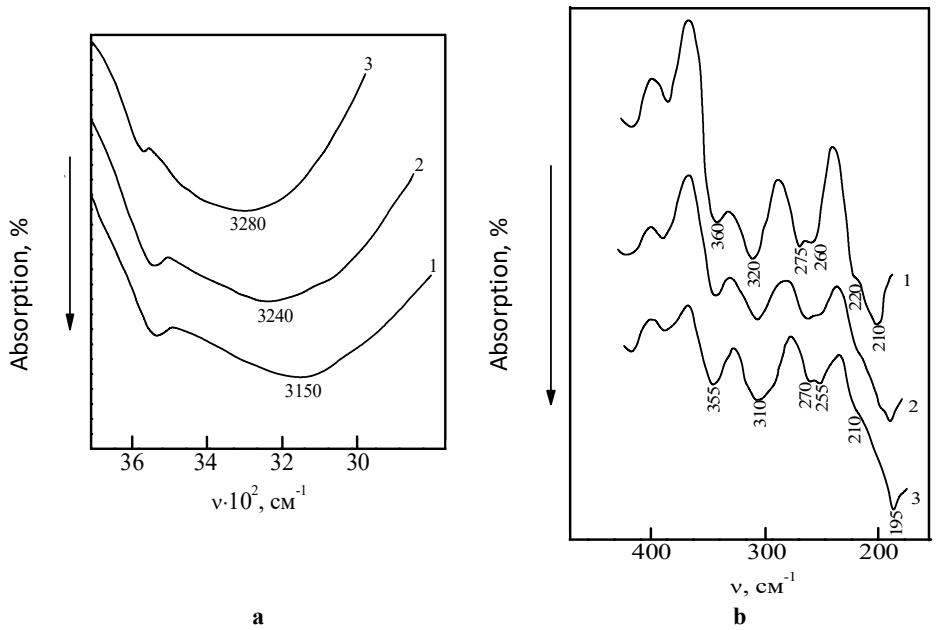

Figure 2. IR spectra of $Zn_2Co(PO_4)_2 \cdot 4H_2O$ (1), $Zn_{2.5}Co_{0.5}(PO_4)_2 \cdot 4H_2O$ (2) and $Zn_3(PO_4)_2 \cdot 4H_2O$: a – in the ν(OH) region, b – in the low-frequency spectral regions (samples were applied to CaF_2). 3150 cm^{-1}, 3240 cm^{-1}, 3280 cm^{-1} – the maximums of the long-wave band ν(OH).

Fluctuations of the cationic sublattice

In addition to the shift in the frequencies of the valence vibrations of the OH groups of water molecules in the IR spectra of zinc-cobalt phosphates of the composition $Zn_{3-x}Co_x(PO_4)_2 \cdot 4H_2O$ in the low-frequency region (350–180 cm^{-1}), a shift of the absorption bands is recorded, which, according to (Bernardino et al., 2022), characterize the oscillations of the cationic sublattice (Figure 2b). When going from $Zn_3(PO_4)_2 \cdot 4H_2O$ to $Zn_2Co(PO_4)_2 \cdot 4H_2O$, a shift in absorption frequencies is observed from 310, 270, 255, 210, 195 cm^{-1} to 320, 275, 260, 225, 210 cm^{-1}, respectively, which agrees with the decrease in atomic mass phosphates, which is 458.11 for $Zn_3(PO_4)_2 \cdot 4H_2O$ and 451.69 for $Zn_2Co(PO_4)_2 \cdot 4H_2O$.

State of the phosphate anion in the structure of zinc-cobalt(II) phosphates

In the region of skeletal vibrations (400–1200 cm^{-1}) in the IR spectra of $Zn_{3-x}Co_x(PO_4)_2 \cdot 4H_2O$ phosphates, valence (800–1200 cm^{-1}) and deformation (500–650 cm^{-1}) vibrations of the PO_4 anion are well separated (Bartl, 2020). The effect of the nature of the cation on the internal vibrations of the phosphate tetrahedron is practically not revealed, since, according to the structural data (Whitaker, 1995), only two oxygen vertices of each octahedron are common with PO_4 tetrahedral. Phosphorus atoms and all its coordinating oxygen atoms are in general positions, that is, the local symmetry of the anion PO_4 – C_1. The correlation scheme constructed for the PO_4 anion taking into account the D_{2h}^{16} factor group ($Zn_{3-x}Co_x(PO_4)_2 \cdot 4H_2O$ crystallizes in the space group D_{2h}^{16} or P_{nma}) looks like this (Figure 3):

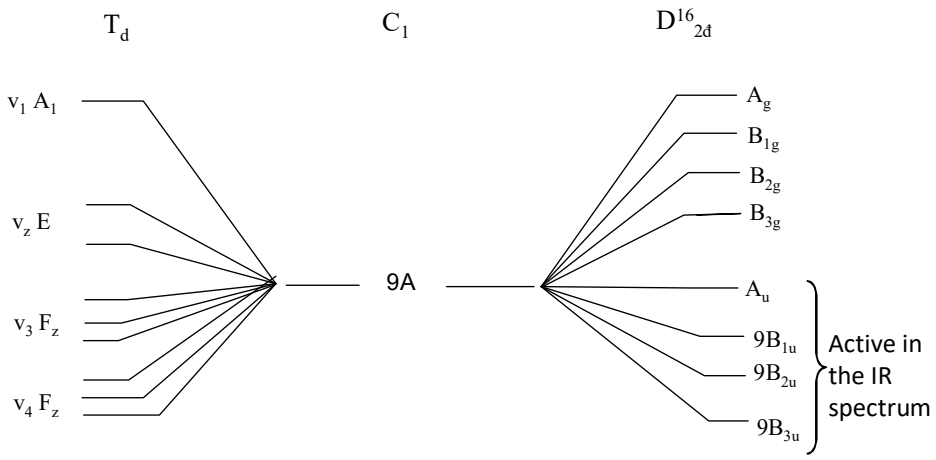

Figure 3. Correlation scheme for PO_4 anion (factor group D_{2h}^{16})

Based on this scheme, the number of frequencies that correspond to the internal vibrations of the PO_4 anion should be equal to 27. At room temperature, it was possible to register 9 bands, at –190 °C – 13; of them, 5 are in the ν_3 bands (out of 9 calculated), 2 are in ν_1 (out of 3 calculated), 2 are in ν_4 (out of 9 calculated), and 4 are in the ν_2 band (out of 6 calculated) (Figure 1). The discrepancy between the calculated and experimental number of bands for the vibrations of the PO_4 tetrahedron is explained by the coincidence of some vibration frequencies of different bonds (Bartl, 2020).

Quite significant splitting of the main absorption bands of the phosphate anion, the appearance of fully symmetric oscillation $\nu_1(A_1)$ – 940, 930 cm^{-1} and ν_2 (E) – 500 and 420 cm^{-1}, usually inactive in IR spectra (Koleva et al., 2018), indicates significant distortions of the tetrahedron in the lattice zinc-cobalt phosphates. This is confirmed by the data of X-ray structural analysis and the interaction of anions with each other due to the presence of hydrogen bonds (Petersen et al., 2022).

Study of process and products of dehydration of zinc-cobalt phosphates during heating

Process and products of dehydration of zinc phosphate tetrahydrate

The heating of $Zn_3(PO_4)_2 \cdot 4H_2O$ is accompanied a decrease in the intensity of the band of valence vibrations of OH-groups of water molecules (3250 cm^{-1}). That occurs in three stages corresponding to the temperature ranges: 65–80, 85–115, and 210–250 °C (Figure 4 b, curve 1). In the spectrum obtained at 85 °C, the intensity of the band with a maximum at 3540 cm^{-1} decreases, and the frequency of the main absorption band (3250 cm^{-1}) shifts to 3390 cm^{-1} in the high-frequency region of the spectrum (Figure 4 a, II).

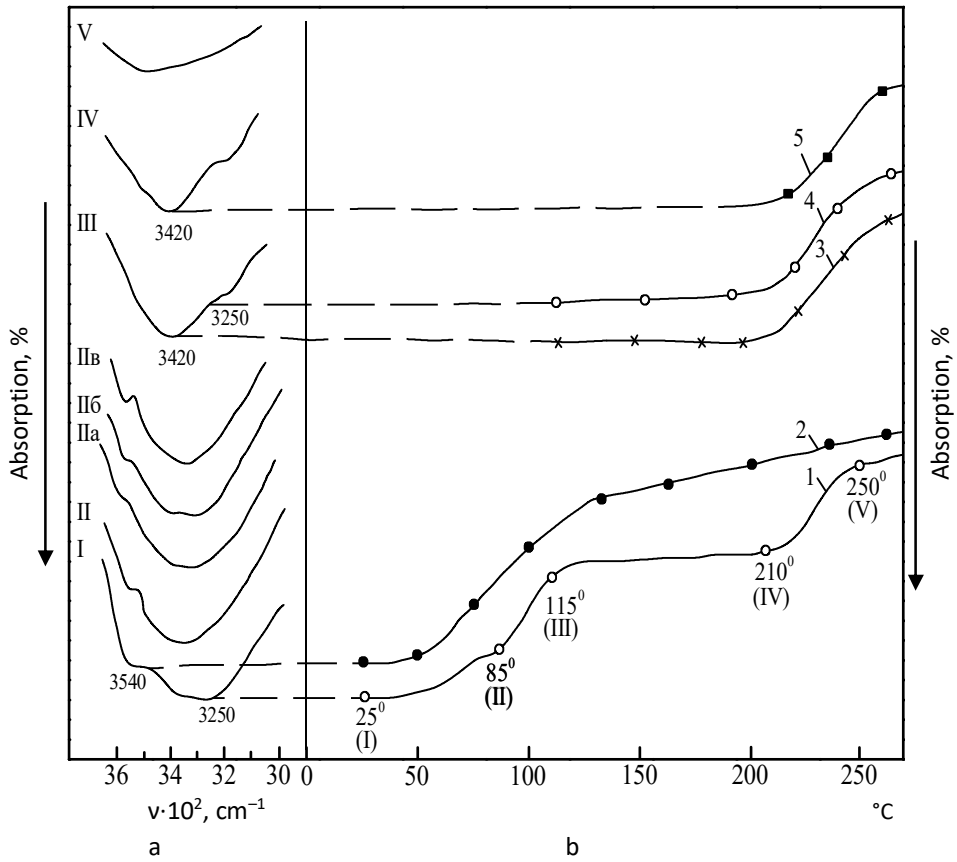

Figure 4. IR spectra of $Zn_3(PO_4)_2 \cdot 4H_2O$ and its dehydration products:
a – ν(OH) bands of water molecules recorded at 25(I), 85(II), 115(III), 210(IV) and 250 °C (V);
II a – ν(OH) of the sample (25 °C) cooled to 85 °C,
II b and II c – ν(OH) 1 and 2 hours after cooling;
b – change in intensity of bands ν(OH) 3250 (1), 3450 (2), 3240 (3), 3250 (4), 3420 cm^{-1} (5)

After cooling the sample to room temperature, the maximum of the main absorption band ν(OH) broadens and again shifts towards low frequencies (3280-3380 cm^{-1}). From the side of the high-frequency wing of the absorption curve, a shoulder at 3540 cm^{-1} is clearly visible, which becomes even more evident in the IR spectrum recorded 1 and 2 hours after the sample has cooled to room temperature (Figure 4a, IIa, IIb, IIc). The main absorption band of 3280-3380 cm^{-1} narrows, and a maximum of 3320 cm^{-1} is more clearly registered. Similar changes in the spectrum of heated to 85 °C and cooled $Zn_3(PO_4)_2 \cdot 4H_2O$ indicate, according to (Anushya et al., 2021), that water removal does not occur in the range of 65–80 °C. This correlates with the results of the study (Bach et al., 2015), in which it is determined that zinc phosphate is stable when heated to 90-100 °C (depending on the heating conditions).

The second stage of a fairly sharp drop in absorption intensity begins at 90 °C (Figure 4 b). The spectrum of $Zn_3(PO_4)_2 \cdot 4H_2O$, recorded at 115 °C, the temperature corresponding

to the beginning of the section of almost constant intensity ν(OH), differs sharply from the spectrum of the original tetrahydrate in the configuration of the absorption band as a whole (Figure 4, curve I, 3). It is characterized by a maximum at 3420 cm^{-1} and a broad shoulder at 3250 cm^{-1} on the low-frequency side of the spectrum. Its identification, made according to known spectroscopic data (Nakamoto, 2009), showed that the product of partial dehydration of $Zn_3(PO_4)_2 \cdot 4H_2O$ is its dihydrate (Anushya et al., 2021).

Therefore, in the range of 90–115 °C, two molecules of the least tightly bound water are removed. The formed dihydrate is stable in a wide range of temperatures (115–210 °C), as evidenced by the IR spectra recorded under these conditions (Figure 4, curves 3, 4, III, IV). This is also mentioned in the work (Bach et al., 2015).

Removal of water from the dihydrate begins at 210 °C and ends at 250 °C. On the curve reflecting changes in the absorption intensity of peaks 3420 and 3250 cm^{-1}, this process corresponds to one step in the range of 210–250 °C (Figure 4 b, curves 3-5). The IR spectrum recorded in the entire range of ν(OH) at 250 °C indicates that heating $Zn_3(PO_4)_2 \cdot 4H_2O$ to 250 °C leads to its almost complete dehydration. This correlates with the results of thermoanalytical studies (Bila et al., 2016), according to which during the heat treatment of zinc phosphate tetrahydrate in the range of 260–280 °C, anhydrous zinc phosphate is formed.

Therefore, the process of dehydration of $Zn_3(PO_4)_2 \cdot 4H_2O$ occurs in two stages with the formation of one stable hydrated form as an intermediate product is the dihydrate of the composition $Zn_3(PO_4)_2 \cdot 2H_2O$.

Process and products of dehydration of zinc-cobalt phosphates

Dehydration of phosphate of composition $Zn_2Co(PO_4)_2 \cdot 4H_2O$, in the crystal lattice of which all octahedral positions are occupied by cobalt, in general, occurs analogously to thermal dehydration of $Zn_3(PO_4)_2 \cdot 4H_2O$ (Figure 5). However, in the course of the curve, which registers the change in the intensities of the maxima of the absorption bands ν(OH) 3150 and 3530 cm^{-1} during the heating process, cancellations are observed.

The intensity of both bands present in the ν(OH) region in the IR spectrum of $Zn_2Co(PO_4)_2 \cdot 4H_2O$ at 90 °C begins to decrease almost simultaneously and ends at 125 °C. A sharp change in absorption intensity occurs in one step, which is equal in magnitude to the first two steps, which are registered in the case of $Zn_3(PO_4)_2 \cdot 4H_2O$ dehydration.

The spectrum of $Zn_2Co(PO_4)_2 \cdot 4H_2O$, recorded in the ν(OH) region at 125 °C, is characterized by a maximum at 3400 cm^{-1} and a shoulder at 3180 cm^{-1} (Figure 5 a, II). It is similar to the spectrum of $Zn_2Co(PO_4)_2 \cdot 2H_2O$ dihydrate obtained under thermography conditions and recorded at room temperature (Anushya et al., 2021). That is, in the interval of 90-125 °C, two water molecules are removed with the formation of a dihydrate of the composition $Zn_2Co(PO_4)_2 \cdot 2H_2O$, which corresponds to one degree on the curve of change in absorption intensity ν(OH).

The same process during the dehydration of $Zn_3(PO_4)_2 \cdot 4H_2O$ is registered by two degrees of decrease in absorption intensity, the first of which is associated with the breaking of H-bonds in the structure preceding the removal of water (Bernardino et al., 2022).

The absence of such a degree when $Zn_2Co(PO_4)_2 \cdot 4H_2O$ is heated is explained by the greater strength of H-bonds realized by OH-groups of water molecules in its structure. The energies of these bonds in $Zn_2Co(PO_4)_2 \cdot 4H_2O$ are most likely close to the energy of bonds between water molecules and the cation (Bartl, 2020). That is why, during the removal of water from $Zn_2Co(PO_4)_2 \cdot 4H_2O$ tetrahydrate, there are no differences in the breaking energy of hydrogen bonds of OH groups and Me-OH_2 bonds.

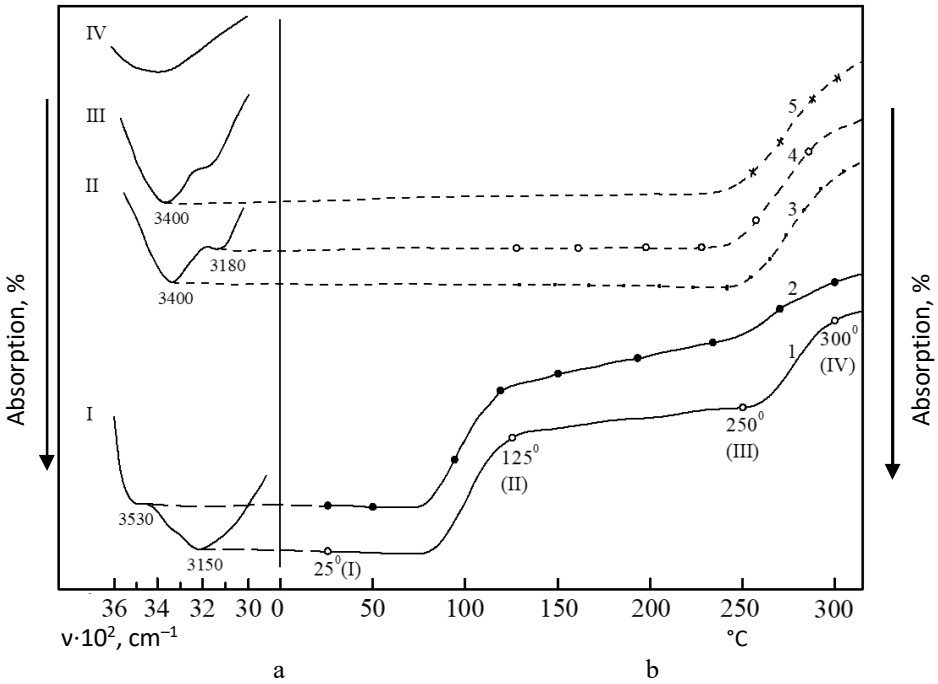

Figure 5. IR spectra of $Zn_2Co(PO_4)_2 \cdot 4H_2O$ and its dehydration products: a – ν(OH) bands recorded at 25(I), 125(II), 250(III) and 300 °C (IV); b – change in intensity of band maxima ν(OH) 3150 (1), 3532 (2), 3400 (3), 3180 (4), 3400 cm^{-1} (5)

The formed $Zn_2Co(PO_4)_2 \cdot 2H_2O$ dihydrate is stable in a wide range temperature (125–250 °C), as evidenced by the spectra taken at these temperatures (Figure 5 a, II, III).

Further heating of $Zn_2Co(PO_4)_2 \cdot 4H_2O$ (above as 250 °C) causes the appearance of a second, less sharp decrease in the intensity of the absorption bands in the range of 250-300 °C (Figure 5 a, curves 3, 4). The ν(OH) bands in the IR spectrum of the sample recorded at 300 °C are practically absent. That is, the removal of two water energy state of water molecules differs insignificantly (Bartl, 2020).

Influence of the nature of the cation on the process and products of dehydration of zinc-cobalt phosphates

In full compliance with the above, dehydration of $Zn_{2.5}Co_{0.5}(PO_4)_2 \cdot 4H_2O$ occurs, a tetrahydrate whose coordination polyhedral in the unit cell contain equal amounts of zinc and cobalt. The nature of the curve of changes in the intensities of the main absorption bands in the ν(OH) region during its heating contains elements characteristic of the dehydration of both $Zn_3(PO_4)_2 \cdot 4H_2O$ and $Zn_2Co(PO_4)_2 \cdot 4H_2O$. A similar effect was noted in work (Yagofarov et al., 2023)

The first stage of water removal is characterized by two degrees of decrease in the absorption intensity of ν(OH) that are less clear than for $Zn_3(PO_4)_2 \cdot 4H_2O$. One of them

characterizes the rupture of hydrogen bonds in the $Zn_{2.5}Co_{0.5}(PO_4)_2 \cdot 4H_2O$ structure (75-90 °C) and is analogous to the dehydration of $Zn_3(PO_4)_2 \cdot 4H_2O$. The second stage is associated with the breaking of Me-OH_2 bonds and the removal of two water molecules (Bartl, 2020). The IR spectrum of the sample obtained at 120 °C and 220 °C is similar to the spectra of dihydrates obtained in the work (Anushya et al., 2021).

The second stage of water removal is registered on the curve of intensity drop ν(OH) by one step. The spectrum of the sample heated to 260 °C corresponds to the completely dehydrated product. It is similar to the IR spectrum of the known anhydrous zinc phosphate (Bach et al., 2015) except for the temperature regimes of formation.

The effect of the nature of the cation is manifested in the stronger polarization effect of cobalt(II) on coordinatively bound water (Antraptseva et al., 2020). As a result, in tetrahydrates, the breaking energy of H-bonds realized by OH-groups of water molecules and M–OH_2 bonds becomes comparable.

The thermal stability of phosphates correlates with the energy state of water molecules and is maximum in phosphates of the composition $Zn_2Co(PO_4)_2 \cdot 4H_2O$ and products of its partial and complete dehydration. The temperature ranges of their formation and thermal stability are 15–20 °C higher than those of phosphates with a lower cobalt content.

So, it was shown that the dehydration of zinc-cobalt phosphate tetrahydrates of the composition $Zn_{3-x}Co_x(PO_4)_2 \cdot 4H_2O$ ($0 \leq x \leq 1.0$) occurs in two stages with the formation of one hydrate form as an intermediate product is a stable dihydrate of the composition $Zn_{3-x}Co_x(PO_4)_2 \cdot 2H_2O$.

Conclusions

1. In the structure of the zinc-cobalt(II) phosphates of the composition $Zn_{3-x}Co_x(PO_4)_2 \cdot 2H_2O$ ($0 < x \leq 1.00$) there are two types of crystallographically non-identical water molecules, the OH-groups of which form a rigid system of hydrogen bonds connections of different strength and direction.
2. The energy of H-bonds, M^{II}–O (OH_2) and P–OH bonds and the asymmetry of water molecules increase with increasing cobalt content in zinc-cobalt phosphates.
3. Dehydration of zinc-cobalt phosphates occurs in two stages with the pairwise removal of water molecules and the formation as an intermediate product of one hydrated form – a stable dihydrate of the composition $Zn_{3-x}Co_x(PO_4)_2 \cdot 2H_2O$.
4. Dehydration temperature regimes correlate with the energy state of water molecules and are maximal in phosphate of the composition $Zn_2Co(PO_4)_2 \cdot 4H_2O$ and products of its partial and complete dehydration. The temperature intervals of their formation and thermal stability are 15–20 °C higher than those of phosphates with a lower cobalt content.

References

Acton A.Q. (2013), *Phosphates – advances in research and application,* Scholarly Editions, Atlanta, Georgia.

Antraptseva N., Solod N., Kochkodan O., Kravchenko O. (2022), Co-precipitation of cations of zinc and divalent metals from phosphoric acid solutions, *Functional Materials,* 29(4), pp. 597–604, https://doi.org/110.15407/fm29.04.597

Antraptseva N., Solod N., Kravchenko O. (2020), Influence of crystal hydrate water on the process and products of heat treatment of magnesium-manganese(II) of dihydrogen phosphates, *Functional Materials,* 27(4), pp. 820–826, https://doi.org/10.15407/fm27.04.820

Anushya G., Freeda T.H. (2021), Thermal parameters of undoped and medicines doped calcium hydrogen phosphate dihydrate and magnesium ammonium phosphate hexahydrate crystals, *Journal of Thermal Analysis and Calorimetry,* 146(5), pp. 1983–1989, https://doi.org/10.1007/s10973-021-10638-0.

Bach S., Celinski V.R., Dietzsch M., Panthofer M., Bienert R., Emmerling F., Schmedt auf der Gunne J., Tremel W. (2015), Thermally highly stable amorphous zinc phosphate intermediates during the formation of zinc phosphate hydrate, *Journal of the American Chemical Society*, 137, pp. 2285-2294, https://doi.org/10.1021/ja5103663

Bartl H. (2020), Water of crystallization and its hydrogen-bonded crosslinking in vivianite $Fe_3(PO_4)_2 \cdot 8H_2O$; a neutron diffraction inwestigation, *Journal of Analytical Chemistry,* 333, pp. 401–403, https://doi.org/10.1007/BF00572335

Bernardino K., Ribeiro Mauro C.C. (2022), Hydrogen-bonding and symmetry breaking in the protic ionic liquid 1-ethylimidazolium nitrate, *Vibrational Spectroscopy,* 120, pp. 103358, https://doi.org/10.1016/j.vibspec.2022.103358

Bila G.N., Antraptseva N.M., Povshuk V.V. (2016), Study of the composition of heat treatment products of manganese(II)-zinc dihydrogen phosphates, *Scientific Works, University of Food Technologies,* 63, pp. 142–147, https://doi.org/10.30888/2663-5712.2022-13-01-014

Damodaran S., Parkin K. L. (2017), *Fennema's Food Chemistry*, CRC Press, Taylor & Francis Group, https://doi.org/10.1201/9781315372914

Goemaere O., Glorieux S., Govaert M., Steen L., Fraeye I. (2021), Phosphate elimination in emulsified meat products: Impact of protein-based ingredients on quality characteristics, *Foods*, 10(4), pp. 882, https://doi.org/10.3390/foods10040882

Grabowski S. (2016), *Hydrogen bonding – new insights*, Springer.

Jurado J.F., Vargas-Hernández C., Vargas R.A. (2012), Raman and structural studies on the high-temperature regime of the KH_2PO_4-$NH_4H_2PO_4$ system, *Revista Mexicana de Física*, 58(5), pp. 411-416, http://www.redalyc.org/articulo.oa?id=57025089005

Koleva V., Stefov V. (2018), Phosphate ion vibrations in dihydrogen phosphate salts of the type $M(H_2PO_4)_2 \cdot 2H_2O$ (M = Mg, Mn, Co, Ni, Zn, Cd): spectra-structure correlations, *Vibrational Spectroscopy*, 64, pp. 89–100, https://doi.org/10.1016/j.vibspec.2018.11.004

Koleva V., Stefov V., Cahil A., Najdoski M., Šoptrajanov B., Engelen B., Lutz H.D. (2019), Infrared and Raman studies of manganese dihydrogen phosphate dihydrate, $Mn(H_2PO_4)_2 \cdot 2H_2O$. I: Region of the vibrations of the phosphate ions and external modes of the water molecules, *Journal of Molecular Structure,* 917(2-3), pp. 117–124, https://doi.org/10.1016/j.molstruc.2019.09.001

Miller D.D. (2010), Food nanotechnology: New leverage against iron deficiency, *Nature Nanotechnoljgy,* 5(5), pp. 318–319, https://doi.org/10.1038/nnano.2010.91

Miller D. (2017), Minerals, In: Damodaran S., Parkin K.L. (Eds.), *Fennema's Food Chemistry*, Boca Raton, CRC Press, https://doi.org/10.1201/9781315372914

Nakamoto K. (2009), Infrared and Raman spectra of inorganic and coordination compounds, Part B. Applications in coordination, organometallic, and bioinorganic chemistry, Jonh Wiley & Sons, Inc, https://doi.org/10.1002/9780470405888

Long N.H.B.S., Gál R., Buňka F. (2011), Use of phosphates in meat products, *African Journal of Biotechnology,* 10(86), pp. 19874-19882, https://doi.org/10.5897/AJBX11.023 ISSN 1684–5315

Petersen H., Stegmann N., Fischer M., Zibrowius B., Radev I., Philippi W., Schmidt W., Weidenthaler C. (2022), Crystal structures of two titanium phosphate-based proton conductors: Ab initio structure solution and materials properties, *Inorganic Chemistry*, 61(5), pp. 2379–2390, https://doi.org/10.1021/acs.inorgchem.1c02613

Pinton M.B., Correa L.P., Facchi M.M.X., Heck R.T., Leães Y.S.V., Cichoski A.J., Lorenzo J.M., Dos Santos M., Pollonio M.A.R., Campagnol P.C.B. (2019), Ultrasound: A new approach to reduce phosphate content of meat emulsions, *Meat Science*, 152, pp. 88–95, https://doi.org/10.1016/j.meatsci.2019.02.010

Scoog D.A., West D.M., Holler F.J. (1992), *Fundamentals of Analytical Chemistry*, Sunders college publ., Boston.

Shao J.H., Deng Y.M., Jia N., Li R.R., Cao J.X., Liu D.Y., Li J.R. (2016), Low-field NMR determination of water distribution in meat batters with NaCl and polyphosphate addition, *Food Chemistry*, 200, pp. 308–314, https://doi.org/10.1016/j.foodchem.2016.01.013

Stabnikova O., Danylenko S., Kryzhska T., Shang F., Zhenhua D. (2022), Effects of different phosphate content on the quality of wheat bran chicken sausage, *Ukrainian Food Journal,* 11(4), pp.588–600, https://doi.org/10.24263/2304-974X-2022-11-4-8

Stabnikova O., Marinin A., Stabnikov V. (2021), Main trends in application of novel natural additives for food production, *Ukrainian Food Journal*, 10(3), pp. 524–551, https://doi.org/10.24263/2304-974X-2021-10-3-8

Tiwari A., Raj B. (2015), Reactions and mechanisms in thermal analysis of advanced materials, Scrivener Publishing LLC, 592 p., https://doi.org/10.1002/9781119117711.

Trojan M., Brandova D. (2010), Study of thermal dehydratation of $Co_{1/2}Mg_{1/2}(H_2PO_4)_2{\cdot}3H_2O$, *Thermochimica Acta*, 159, pp. 1–12, https://doi.org/10.1016/j.tca.2010.10.003

Wang P., Xu X., Zhou G. (2009), Effects of meat and phosphate level on water-holding capacity and texture of emulsion-type sausage during storage, *Agricultural Sciences in China*, 8(12), pp. 1475–1481, https://doi.org/10.1016/s1671-2927(08)60361-2

Whitaker A. (1995), The crystal structure of hopeite, *Acta Crystallographica,* 31(8), pp. 2026–2035, https://doi.org/10.1107/S0567740878008286

Wu W. Y., Liang X. Q., Li Y. Z. (2015), $CoZn_2(PO_4)_3{\cdot}4H_2O$, a cobalt-doped modifications of hopéite, *Acta Crystallographica,* E 61, pp. 105–107, https://doi.org/10.1107/S1600536805014078

Xu L., Lv Y., Su Y., Chang C., Gu L., Yang Y., Li J. (2021), Enhancing gelling properties of high internal phase emulsion-filled chicken gels: Effect of droplet fractions and salts, *Food Chemistry*, 367, 130663, https://doi.org/10.1016/j.foodchem.2021.130663

Yagofarov M. I., Sokolov A.A., lya S. Balakhontsev I.S., Nizamov I.I., Solomonov B.N. (2023), Thermochemistry of fusion, solution and hydrogen bonding in benzamide, *N*-methylbenzamide, and acetanilide, *Thermochimica Acta*, 728, pp. 179579-179586, https://doi.org/10.1016/j.tca.2023.179579

Zimmermann M.B., Hilty F.M. (2011), Nanocompounds of iron and zinc: Their potential in nutrition, *Nanoscale*, 3(6), pp. 2390–2398, https://doi.org/10.1039/c0nr00858c